

# Morphological variations and dysmorphic features in the sea cucumber *Cucumaria frondosa*

Guillaume Corbisier<sup>ip,a,b</sup>, Kevin C.K. Ma<sup>a</sup>, Sara M. Jobson<sup>a</sup>, Jean-François Hamel<sup>c</sup>, Guillaume Caulier<sup>b</sup>, and Annie Mercier<sup>a</sup>

<sup>a</sup>Department of Ocean Sciences, Memorial University, St. John's, Newfoundland and Labrador, Canada; <sup>b</sup>Biology of Marine Organisms and Biomimetics Unit, Research Institute for Biosciences, University of Mons, Belgium; <sup>c</sup>Society for the Exploration and Valuing of the Environment (SEVE), St. Philips, Newfoundland and Labrador, Canada

Corresponding authors: Annie Mercier (email: [amercier@mun.ca](mailto:amercier@mun.ca)); Guillaume Corbisier (email: [guillaume.corbisier@alumni.umons.ac.be](mailto:guillaume.corbisier@alumni.umons.ac.be))

## Abstract

Studying morphological abnormalities provides valuable insights into the developmental processes, species adaptability, gene expression, and the potential effect of environmental pressures. Dysmorphic features are well known within several taxa like arthropods but has much less been investigated in others like echinoderms, and specially sea cucumbers (Holothuroidea). The dendrochirotid *Cucumaria frondosa* (Gunnerus, 1767), which is the most studied and economically important holothuroid species in the North Atlantic, is known to present different colour morphotypes but anatomical variations have rarely been reported. This study tallied dysmorphic features across a sample of more than 900 individuals of *C. frondosa* examined over five years. About 1.3% and 15.9% of individuals presented non-standard external or internal anatomical characteristics, respectively. Individuals with unusual body plans, including two posterior ends and two cloaca/anuses, or an abnormal number of tentacles, were discovered. Others exhibited supernumerary organs, or organs of unusual shape and size, e.g., ramified/split ambulacra and longitudinal muscle bands, ramified or supernumerary Polian vesicles, hypertrophied madreporites, inter-vesicle protrusions, and hypertrophied circular haemal vessels. These features are described here for the first time in *C. frondosa* and have not been reported before in holothuroids. The severity of the morphological changes along with their possible drivers and impacts is discussed.

**Key words:** phenotypic variations, dysmorphology, Echinodermata, dendrochirotid, sea cucumber, *Cucumaria frondosa* (Gunnerus, 1767)

## Résumé

L'étude des anomalies morphologiques apporte des précieuses informations sur le développement, l'adaptabilité des espèces, l'expression des gènes ainsi que l'effet potentiel que peuvent avoir les pressions environnementales. Les dysmorphies, bien connues chez certains taxa comme les arthropodes, sont peu étudiées chez les échinodermes, notamment les concombres de mer (Holothuroidea). Le dendrochirote *Cucumaria frondosa* (Gunnerus, 1767), le concombre de mer le plus étudié et économiquement important de l'Atlantique Nord, est connu pour ses morphotypes de couleur, mais ses variations anatomiques ont rarement été documentées. Cette étude analyse les anomalies chez plus de 900 individus de *C. frondosa* examinés sur cinq ans. Environ 1,3% et 15,9% des spécimens présentaient des anomalies externes ou internes, respectivement. Certains affichaient des schémas corporels inhabituels, tels que deux cloaques ou un nombre anormal de tentacules, tandis que d'autres avaient des organes surnuméraires ou de forme atypique, comme des canaux ambulacrariaires et bandes musculaires ramifiées, des madréporites hypertrophiées, ou des vésicules de Poli surnuméraires. La plupart de ces anomalies, inédites chez *C. frondosa*, n'ont jamais été décrites chez les holothurides. La gravité de ces changements morphologiques, ainsi que leurs causes et impacts potentiels, sont discutés. [Ceci est une traduction fournie par l'auteur du résumé en anglais].

**Mots-clés :** variations phénotypiques, dysmorphologie, Echinodermata, Dendrochirotes, concombre de mer, *Cucumaria frondosa* (Gunnerus, 1767)

## Introduction

Dysmorphology is the measurement of morphological abnormalities, including unusual shapes, sizes, and arrange-

ments of body parts that differ from what is typically documented in a species (Claes et al. 2012). This definition implies that morphological abnormalities are normally scarce

and can only exist if prior knowledge of what is standard or typical has previously been well defined. Studying dysmorphology offers insights into developmental processes, gene expression, environmental effect, and adaptability within species. It can reveal how organisms respond to environmental pressures or stressors and contribute to understanding phenotypic plasticity and resilience (Whitman and Agrawal 2009).

Among invertebrates, malformations and morphotype dissimilarities are the subject of comprehensive research in the phylum Arthropoda, principally on insects (Malcomson 1953; Adamski et al. 2005; Leśniewska et al. 2009), crustaceans (Scholtz 2020), or pycnogonids (Utinomi 1971; Flandroit et al. 2024). Morphological variability in echinoderms has been documented to a lesser extent, chiefly as case studies (e.g., Dafni 1980; Stewart and Mladenov 1997; Candia Carnevali 2005; Mironov et al. 2015; Galván-Villa and Solís-Marín 2021; Roux and Phillippe 2021; Rupp et al. 2024). Moreover, while the scientific literature on echinoderms dates back more than a century and frequently mentions morphological and functional variations (Edwards 1910; Hawkins 1917; Saint-Seine 1950; Roman 1952; Serafy 1971; Smith et al. 1973; Allain 1978; Watts et al. 1983), dysmorphic features were seldom characterised and investigated in detail, particularly in sea cucumbers (class Holothuroidea).

Echinoderms, particularly Echinoidea and Holothuroidea, are recognised as bioindicators and have been investigated in embryo-larval bioassays. Consequently, dysmorphic features have primarily been documented as indicators of teratogenic effects and pollutant-induced disruptions during embryonic/larval development and juvenile growth in ecotoxicological research (Allain 1978; Warnau et al. 1996; Pesando et al. 2003; Carballeira et al. 2012; Morroni et al. 2020, 2023; Wang et al. 2023). Variations in environmental conditions, including salinity and temperature fluctuations, endocrine disruptors, pathogens, error in the regeneration process, and diseases, have also been identified as potential sources of morphological abnormalities (Hotchkiss 1979; Watts et al. 1983; Jangoux 1987; Candia Carnevali 2005; Vergneau-Grosset et al. 2022).

Anatomical discrepancies in sea stars (Asteroidea) relate mostly to the description of unusual arm numbers caused by high salinity, genetic basis, error in regeneration process, and larval development flaw (Hotchkiss 1979; Watts et al. 1983). Whereas in sea urchins (Echinoidea) dysmorphic features involve variations in growth or skeletal morphology, regeneration errors, distortion in the digestive tract, and tissular disorders in adult and larval stages (Allain 1978; Dafni 1980; Candia Carnevali 2005; Carballeira et al. 2012; Xu et al. 2015). In crinoids (Crinoidea), they have been mostly documented from fossils (Stiller 1999; Thomka et al. 2014) and occasionally from living individuals (Candia Carnevali 2005; Eeckhaut and Améziane-Cominardi 2020), in the form of skeletal deformations and regenerative malfunction as a result of epibiotic interactions. Brittle stars (Ophiuroidea) are the subject of the only neoplasm case described in Echinodermata, with individuals of *Ophiocomina nigra* (Abildgaard, 1789) exhibiting tumour-like epiderma (Fontaine 1969; Sparks 2012). Records of non-standard Holothuroidea are particularly scarce and

have principally focused on embryos or larvae, e.g., odd gastrulation and misaligned mesenchymal cells in *Apostichopus japonicus* (Selenka, 1867) (Wang et al. 2023). Other relatively standard phenotypic variations reported in sea cucumbers range from unusual colours of the body wall (Montgomery et al. 2019; Xing et al. 2024) to sexual dimorphism of the genital papillae (McEuen 1988; O'Loughlin 2001; Montgomery et al. 2018). A more striking example was recently presented by Rupp et al. (2024) who described several cases of anteriorly bifurcated ("bicephalic") adult sea cucumbers from various orders, living across temperate and tropical areas: *Holothuria (Halodeima) grisea* Selenka, 1867 in Brazil, *Apostichopus californicus* (Stimpson, 1857) in the United States of America, *Holothuria leucospilota* Brandt, 1835 in La Réunion (France), *Holothuria forskali* Delle Chiaje, 1824 in Spain, and *Parastichopus tremulus* (Gunnerus, 1767) in Norway. These sea cucumbers all possessed two mouths, two aquapharyngeal bulbs, two stomachs, along with examples of duplicated organs. Despite being abnormally constituted, they had reached adulthood and, in some cases, were observed to display typical locomotor and feeding behaviours (Rupp et al. 2024).

The sea cucumber *Cucumaria frondosa* (Gunnerus, 1767) plays a major role in subtidal ecosystems of the Arctic and North Atlantic regions (Gianasi et al. 2021; Mercier et al. 2023), where it is commercially exploited for human consumption and for its pharmaceutical and nutraceutical properties (Hossain et al. 2020; Gianasi et al. 2021; Mercier et al. 2023). This species is by far the most studied cold-water sea cucumber and is among the most fished as well (Gianasi et al. 2021; Mercier et al. 2023). Accordingly, the anatomy of *C. frondosa* has been well studied and described for more than a century (e.g., Edwards 1910; Hamel and Mercier 1996; Nelson et al. 2012; Hossain et al. 2020). However, phenotypic morphological variations in this species have been the subject of few scientific publications. Specifically, Montgomery et al. (2019) highlighted colour variations in the body wall, from the dark brown to orange and white individuals, whereas a blueish individual with white longitudinal and circular muscle bands (normally pink in colour) was described by Mercier et al. (2023).

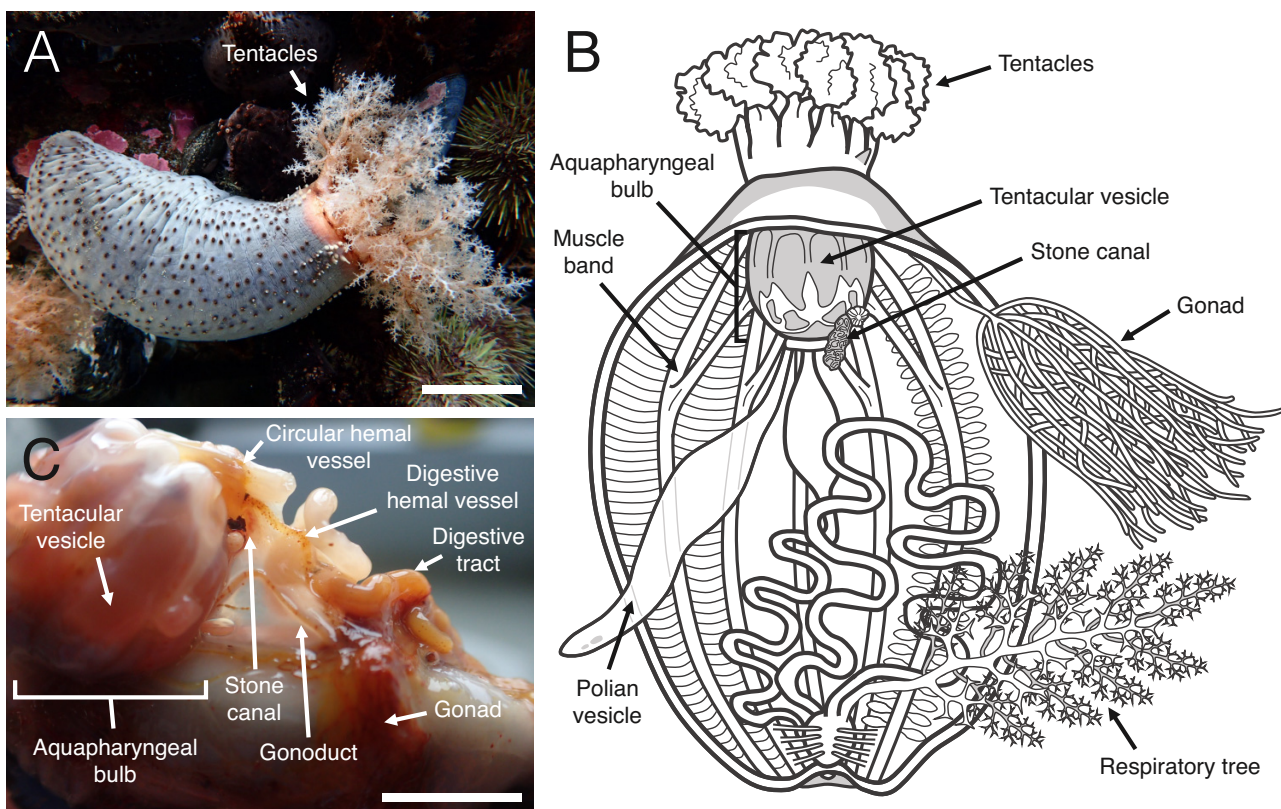
The present study took advantage of ongoing research projects where individuals of *C. frondosa* were examined on a regular basis to make the first comprehensive inventory of the dysmorphic features in an echinoderm species. The aim was to detect and characterise previously undocumented internal and external morphological and morphometric variations in representatives from the Northwest Atlantic. Occurrences, as well as possible causes and consequences of those variations, were detailed and investigated.

## Materials and methods

### Collection and maintenance

A total of 926 adult individuals of the northern sea cucumber *C. frondosa* ranging from 7 to 28 cm in contracted length were collected from two locations in Newfoundland, eastern Canada. Of these, 432 individuals were hand collected by divers from Tors Cove (47°12'44"N; 52°50'39"W) at depths

**Fig. 1.** External and internal anatomy of the sea cucumber *Cucumaria frondosa* (Gunnerus, 1767): (A) external view of an adult individual with tentacles extended, (B) schematic drawing of the general anatomy, and (C) internal view of the aquapharyngeal bulb and surrounding organs; scales bars represent ~30 mm in panel (A) and ~10 mm in panel (C).



of 10–15 m, and 494 individuals were collected by commercial harvesters with a bottom trawl on the St. Pierre Bank ( $46^{\circ}00'00''\text{N}$ ;  $56^{\circ}15'00''\text{W}$ ) at depths of 20–60 m. Sea cucumbers from Tors Cove were obtained between October 2019 and May 2023 and those from the St. Pierre Bank between July 2020 and August 2023.

Permits for field collections were granted by Fisheries and Oceans Canada and all handling procedures followed the Canadian Council on Animal Care guidelines.

## Phenotypes

### External

Morphological and morphometric variations and abnormalities were determined based on the known standard anatomy of *C. frondosa* ( $n = 700$ ; **Fig. 1**) (e.g., [Edwards 1910](#); [Gianasi et al. 2021](#); [Mercier et al. 2023](#)). Live individuals were examined and photographed with an Olympus Tough TG-6 camera to inventory any variant in external phenotype, including different organisation of ambulacra and associated podia, unusual tentacle numbers, and departure from normal body plan (**Fig. 1A**).

### Internal

A total of 226 individuals were investigated for internal variations. The body wall was opened using a surgical scalpel

on the ventral side (i.e., the trivium), from the anus (cloaca) to the mouth between two rows of podia. Then, the body wall was inverted and the exposed organs were measured with a digital calliper, examined under a stereomicroscope (Leica M205 FA), and photographed with a digital camera (Leica DFC7000). Among the features investigated were the Polian vesicle (number, length, volume of fluid, and shape), the stone canal (length and width), the madreporite (number and size), the aquapharyngeal bulb, the ambulacrum (shape), the ampullae of the podia, the circular haemal vessel (size, lumen dimension, fluid volume, and coelomocytes quantity), and the longitudinal muscle bands (**Figs. 1B** and **1C**). Sea cucumbers exhibiting morphological variations were sexed following the methodology developed in [Montgomery et al. \(2018\)](#).

In addition to the number and size (length and width) of the Polian vesicle, the total volume of fluid it held was determined by draining its content into a Petri dish and transferring it to a Falcon tube (50 mL). Results were compared to the volume held in typical forms (i.e., individuals with a single Polian vesicle). The point of insertion of the vesicle(s) along the ring canal was also noted along with their position in relation to each other. To investigate the potential immunological activity of the abnormal inter-vesicle protrusions, their diameter was measured and their internal content was punctured with a syringe mounted with a G21 needle before being analysed to detect potential coelomocytes or coelomocyte aggregates under a light microscope (Nikon Eclipse 80i coupled to an Olympus DP73 camera) following the cellular descrip-

**Table 1.** External and internal morphological variations and abnormalities of the sea cucumber *Cucumaria frondosa*.

Dysmorphic features	Number of individuals investigated	Morphological variations and abnormalities (estimated rate in %)	Associated figure
X- and Y-shaped ambulacrum/muscle band	~400	5 (1.3)	Fig. 2
Variation of tentacle number	~300	3 (1)	Fig. 3
Unusual body plan	~400	1 (0.3*)	Fig. 4
Multiple Polian vesicles	226	18 (8.0)	Fig. 5
Branched Polian vesicle	226	1 (0.4)	Fig. 5
Hypertrophied madreporite	94	12 (12.8)	Fig. 6
Inter-vesicle protrusion	94	1 (1.1)	Fig. 7
Hypertrophied haemal vessel	94	4 (4.3)	Fig. 8

\*The proportion of the population with an unusual body plan is probably lower than 0.3%.

tion made by Caulier et al. (2020). Moreover, the circulation of the hydrovascular fluid between the protrusions and the vesicles of the tentacles could be determined visually following the transfer of red coelomocyte aggregates between the two compartments.

## Results

Among the 926 sea cucumbers examined, 45 instances of morphological variations and abnormalities in both male and female individuals were reported and classified into eight categories (Table 1). Accordingly, 9 out of 700 ( $\pm 1.3\%$ ) and 36 out of 226 ( $\pm 15.9\%$ ) sea cucumbers displayed external and internal morphological variations or abnormalities, respectively (Table 1). No single individual exhibited more than one dysmorphic feature. The hydrovascular system was the most affected. The muscular system, the haemal system, and the body plan (the organisation of some internal organs included) were also impacted, as detailed below.

### External dysmorphic features

#### Body wall

After examining 400 individuals of *C. frondosa* from the St. Pierre Bank collected between 2022 and 2023, most individuals (~98.8%) exhibited typical morphologies (Figs. 2A–2C). Internally, five retractor muscle bands were observable (Fig. 2A) with the arrangement of openings associated with the podia mirrored on the integument (Fig. 2C). Five cases of atypical body walls were observed (Figs. 2D–2I), based on podia organisation along the ambulacrum. Among these, four individuals presented a ramified (i.e., Y-shaped) ambulacrum (Figs. 2E and 2H) towards the posterior end of the body wall, shifting the symmetry of the body from pentaradial to hexaradial. Inwardly, the ambulacra were respectively associated with five (Fig. 2D) or six retractor muscle bands (Fig. 2G), and the arrangement of podia openings followed suit (Fig. 2F). The Y-shaped morphology could be associated with the ambulacrum of both the trivium (Fig. 2E) and the bivium (Fig. 2H). The fifth atypical body wall belonged to an individual with an X-shape ambulacrum and a pentaradial body symmetry, except at the intersection point of the X-shaped ambulacrum

(Fig. 2I). Two rows of podia, forming an X-shape, were discernible externally along the entire length of this atypical ambulacrum. Inwardly, the two longitudinal muscle bands were seemingly fused at the centre, forming an X shape (Fig. 2I). Notably, this individual had four retractor muscle bands, instead of the typical five (Fig. 2I).

#### Number of tentacles

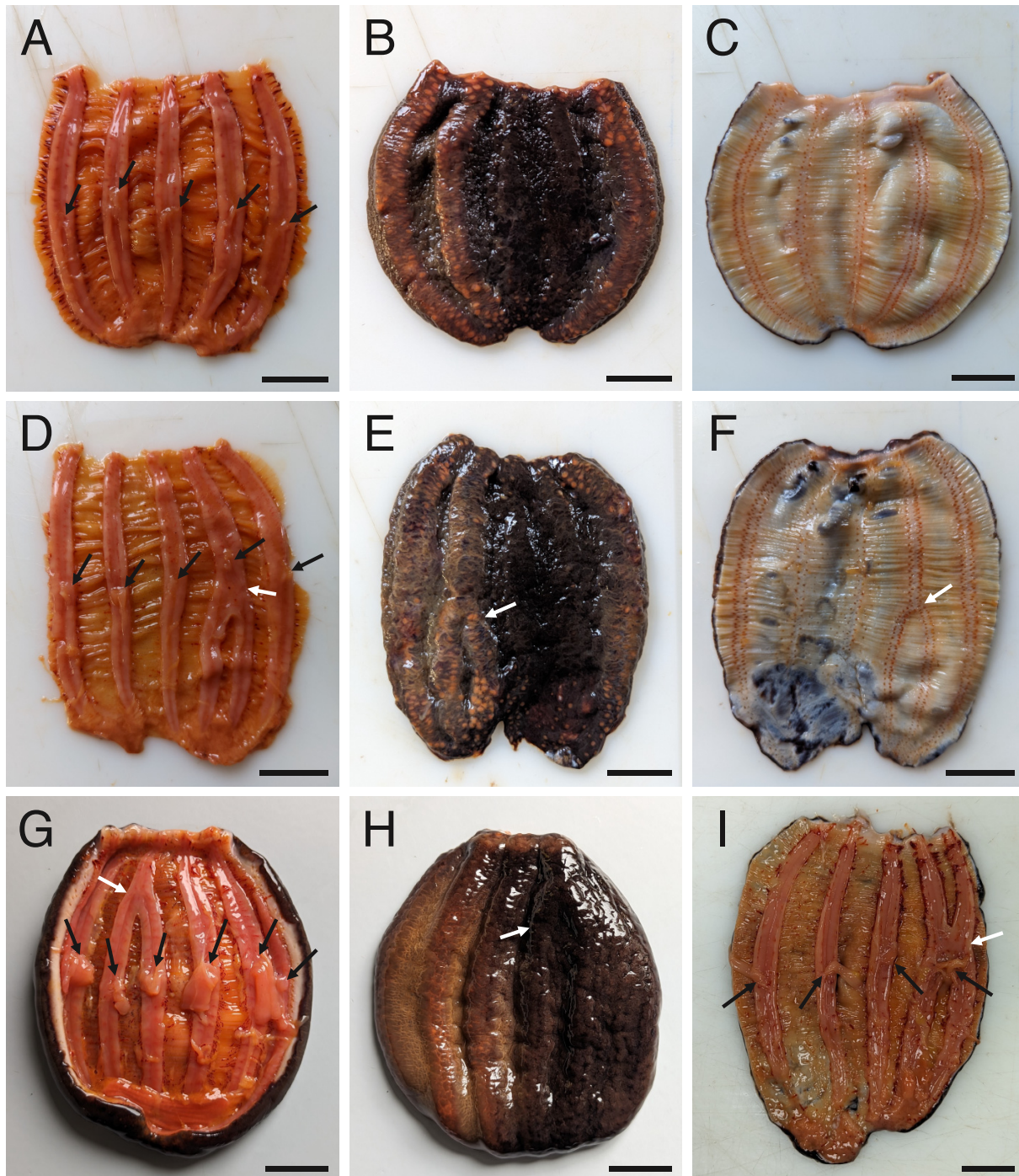
The tentacle numbers of approximately 300 individuals of *C. frondosa* from Tors Cove were inspected, and three individuals (~1%) deviated from the standard 10 (Fig. 3A) with a corresponding number of tentacle vesicles, i.e., two vesicles between any two retractor muscles (Fig. 3B). Two individuals exhibited nine tentacles of equal size (Fig. 3C) and had 10 associated vesicles with typical configuration; however, one of the vesicles was substantially smaller (Fig. 3D). Additionally, one individual presented 11 tentacles of equal size (Fig. 3E) with a corresponding number of vesicles: four sets of two vesicles between two retractor muscles and one set of three vesicles between two retractor muscles (the middle vesicle being larger in size; Fig. 3F).

### Internal dysmorphic features

#### Body plan

One of the 400 individuals collected from the St. Pierre Bank exhibited an atypical external morphology. This individual displayed two posterior ends associated with two cloacal openings (Fig. 4C). The diameter of each cloacal opening was 2.2 mm. The abnormal lateral protrusion was oriented ~40° from the main body. Internally, this individual comprised two separate respiratory trees and cloaca, one set associated with the main body and another with the lateral protrusion (Figs. 4D–4F). The body wall of the main body section consisted of five longitudinal muscle bands; however, one of the muscle bands continued into the body wall of the lateral protrusion (Figs. 4E and 4F); consequently, body symmetry went from pentaradial in the anterior section to quadriradial in the posterior section. The body wall of the lateral protrusion also consisted of the standard five longitudinal muscle bands (Figs. 4E and 4F). Unusually elongated retractor mus-

**Fig. 2.** Typical and atypical body-wall morphologies of the sea cucumber *Cucumaria frondosa* (Gunnerus, 1767): (A) typical longitudinal muscle bands with five retractor muscle bands, (B) typical ambulacra as viewed externally, (C) typical ambulacra and associated podium openings on the integument as viewed internally, (D) atypical Y-shaped longitudinal muscle band with one retractor muscle band, (E) atypical Y-shaped ambulacrum (trivium) as viewed externally, (F) atypical Y-shaped ambulacrum and associated podium openings on the integument as viewed externally, (G) atypical Y-shaped longitudinal muscle band with two retractor muscle bands, (H) atypical Y-shaped ambulacrum (bivium) as viewed externally, and (I) X-shaped longitudinal muscle band(s) with one retractor muscle band; white arrows indicate the atypical longitudinal muscle band morphologies; black arrows indicate attachment points of retractor muscle bands to the longitudinal muscle bands; scale bars represent 20 mm.

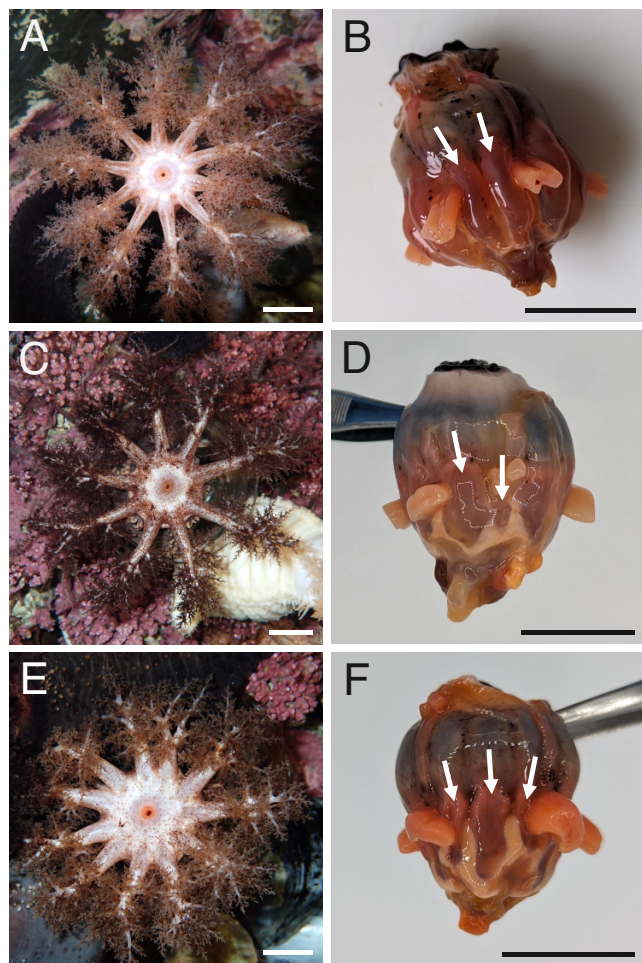


cle bands (about two-thirds the length of the longitudinal muscle band) were present in the main body section (Figs. 4E and 4F).

#### Polian vesicle

Most individuals from Tors Cove (121 individuals out of 132, or 91.7%) exhibited an hydrovascular system with a sin-

**Fig. 3.** Typical and atypical numbers of tentacles and vesicles of the tentacles in the sea cucumber *Cucumaria frondosa* (Gunnerus, 1767): (A) typical individual with 10 tentacles, (B) typical aquapharyngeal bulb with two vesicles of the tentacles between two retractor muscles, (C) atypical individual with nine tentacles, (D) atypical aquapharyngeal bulb associated with an individual with nine tentacles with two vesicles of the tentacles between two retractor muscles but one on the right was substantially smaller in size, (E) atypical individual with 11 tentacles, and (F) atypical aquapharyngeal bulb associated with 11 tentacles with three vesicles of the tentacles between two retractor muscles with the middle vesicle being larger; arrows indicate a vesicle of the tentacle; scale bars represent 20 mm.



single transparent unbranched Polian vesicle full of hydrovascular fluid, attached to the ring canal (Fig. 5A). The Polian vesicle monopolised a considerable section of the perivisceral body cavity; it had an average length of  $126.3 \pm 46.1$  mm and width of  $14.1 \pm 1.7$  mm ( $n = 16$ ). Among the 132 sea cucumbers, 6.8% ( $n = 9$ ) displayed two Polian vesicles, each of which had distinct points of attachment to the ring canal (Figs. 5B and 5C). In addition, one individual (0.8%) had four Polian vesicles: two fully grown ( $\sim 6$ –10 cm in length) and two underdeveloped ( $\sim 1$ –2 cm). Another individual (0.8%) exhibited a single Polian vesicle but with an uncharacteristically

branched morphology (Fig. 5F). The sea cucumbers from the St. Pierre Bank ( $n = 94$ ) yielded eight individuals (8.5%) with multiple Polian vesicles; six had two Polian vesicles (6.4%), one had three (1.1%; Figs. 5D and 5E), and another (1.1%) had six, among which two were fully grown ( $\sim 7$ –8 cm in length) and four were underdeveloped ( $\sim 1$ –2 cm).

For the two populations of *C. frondosa* examined, the position of the single Polian vesicle on the ring canal was the left dorsal inter-radius. However, in the 18 individuals with two or more Polian vesicles, the position of the second vesicle was consistently on the right ventral inter-radius (Fig. 5C). Furthermore, the third Polian vesicle was always ( $n = 3$ ) positioned on the left ventral inter-radius (Fig. 5E). The position of the fourth Polian vesicle ( $n = 2$ ) varied from right to left ventral inter-radius (the latter being next to second or third Polian vesicle). The fifth and six underdeveloped Polian vesicles were observed alongside the fully grown third Polian vesicle.

The total fluid volume within the Polian vesicle was measured in a subsample of individuals possessing two vesicles ( $n = 4$ ) where the cumulative volume (per individual) was  $12.8 \pm 3.2$  mL compared to  $15.7 \pm 5.4$  mL in single Polian vesicles ( $n = 4$ ).

### Madreporite

Among 94 individuals collected between 2020 and 2021 from the St. Pierre Bank, 12 (13%) possessed a hypertrophied madreporite. In the typical morphology, an oval calcareous madreporite with a diameter between 1.5 and 2.5 mm ( $n = 15$ ) is attached to the stone canal (length:  $9.6 \pm 3.4$  mm; width:  $1.8 \pm 0.2$  mm;  $n = 15$ ) (Fig. 6A); the stone canal is connected to the ring canal on the right ventral inter-radius and is red in colour, as its fluid is filled with coelomocytes, in particular haemocytes. Hypertrophied madreporites displayed three different morphologies: a larger elongated madreporite (Figs. 6C and 6D), a large lump alongside a typical madreporite (Fig. 6E), and a larger knobby madreporite (Figs. 6B and 6F). Seven individuals exhibited a madreporite of increased size (i.e., elongated madreporite), measuring  $6.9 \pm 1.9$  mm in length and  $3.6 \pm 0.7$  mm in width and the longest measuring 8.8 mm in length and 4.3 mm in width (Figs. 6C and 6D). Four individuals presented a standard madreporite (diameter:  $\sim 1.5$  mm) alongside a larger madreporite with a diameter of  $4.2 \pm 0.6$  mm (Fig. 6E). The peduncle was divided in two at the third quarter of its length, and each end was distally terminated by a madreporite. The cluster of madreporites was only observed once; it had a diameter of 7 mm as a result of the aggregation of 10 units that each measured  $\sim 2.2$  mm in diameter (Fig. 6F).

Irrespective of the number and size of madreporites, the stone canal length always ranged between 0.6 and 1.2 cm. Independently of the morphology, the hypertrophied and typical madreporites were always internalised inside the perivisceral coelom. The madreporite is run through by wide lacunae. The typical madreporite lacunae varied from  $\sim 10$   $\mu$ m to a maximum of  $\sim 100$   $\mu$ m in width, whereas lacunae in hypertrophied madreporite had a width of  $\sim 10$   $\mu$ m and up to 500  $\mu$ m. Hypertrophied madreporites were covered by cilia-

**Fig. 4.** Posteriorly bifurcated individual sea cucumber *Cucumaria frondosa* (Gunnerus, 1767): (A) external view of the body wall on the dorsal side (bivium), (B) external view of the body wall on the ventral side (trivium), (C) an oblique view of the two cloacal openings, (D) view of some of the internal organs, (E) internal view of the body wall on dorsal view (bivium), and (F) internal view of the body wall on ventral side (trivium); scale bars represent 30 mm.

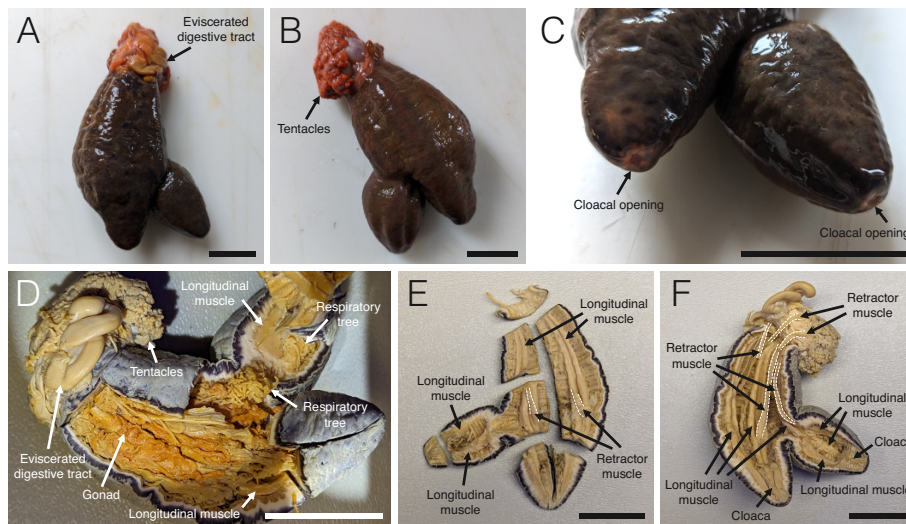
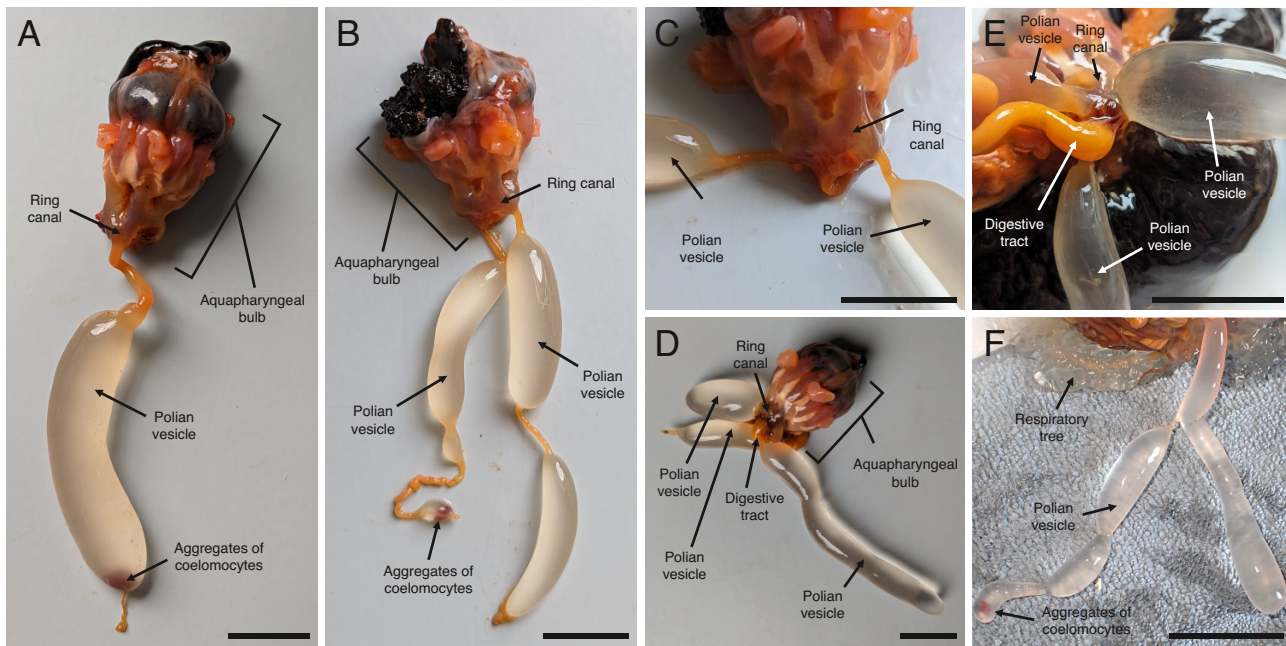


**Fig. 5.** Typical and atypical Polian vesicle morphology in the sea cucumber *Cucumaria frondosa* (Gunnerus, 1767): (A) an individual with one (unbranched) Polian vesicle, (B) an individual with two separate (unbranched) Polian vesicles, (C) view of the attachment points of two Polian vesicles to a ring canal, (D) an individual with three separate (unbranched) Polian vesicles, (E) view of attachment points of three Polian vesicles to a ring canal, and (F) an individual with a branched Polian vesicle; aggregates of coelomocytes (red in colour) are visible towards the distal end of the Polian vesicles in panels (A), (B), and (F); scales bars represent 20 mm.



tion on the surface and inside the lacunae as in any conventional madreporite.

### Vesicle of the tentacles

A unique abnormality was detected on the aquapharyngeal bulb of a single individual from St. Pierre Bank in July

2020. In the area of transition between the ring canal and the vesicle of the tentacle, 12 inter-vesicle protrusions and five deflated inter-vesicle protrusions were present (Figs. 7A and 7B). The diameter of non-deflated protrusions varied from a minimum of 1 mm to a maximum of 4 mm, while the deflated protrusions, filled by haemocytes, each had a diameter of ~4 mm. The cumulative volume of fluid extracted from

**Fig. 6.** Typical and atypical madreporite morphologies in individuals of the sea cucumber *Cucumaria frondosa* (Gunnerus, 1767): (A) typical madreporite and stone canal, (B) hypertrophied, knobby madreporite still attached to the aquapharyngeal bulb, (C and D) hypertrophied, elongated madreporite, (E) hypertrophied madreporite with a smaller lump to the left and a larger one to the right, and (F) hypertrophied, knobby madreporite; scale bars represent 2 mm in panels (A) and (C–F), and 10 mm in panel (B).

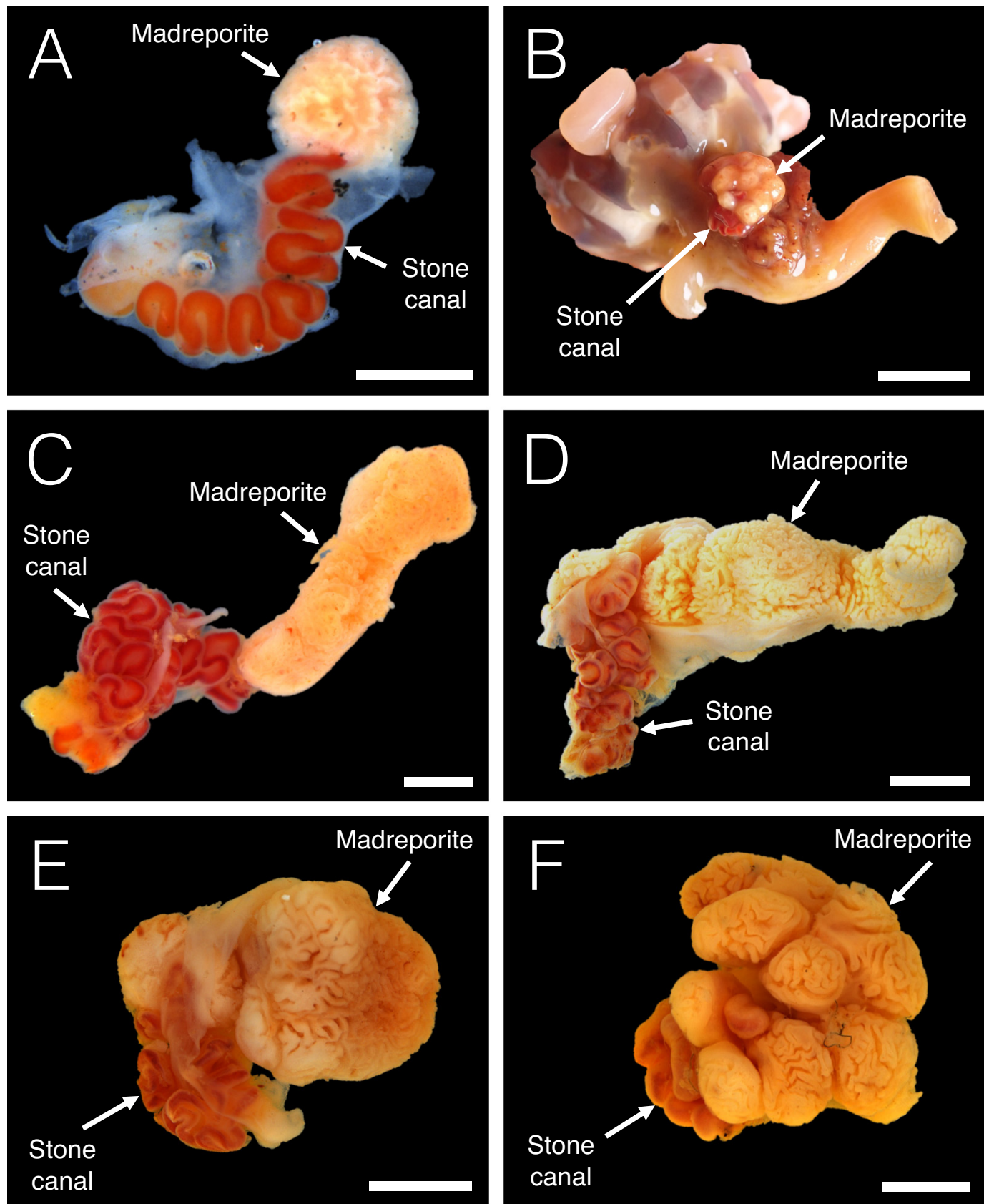


**Fig. 7.** Inter-vesicle protrusions and deflated inter-vesicle protrusions in an individual sea cucumber *Cucumaria frondosa* (Gunnerus, 1767): (A) an atypical aquapharyngeal bulb and (B) a closer view of the inter-vesicle and deflated inter-vesicle protrusions on the aquapharyngeal bulb; scales bars represent 10 mm.

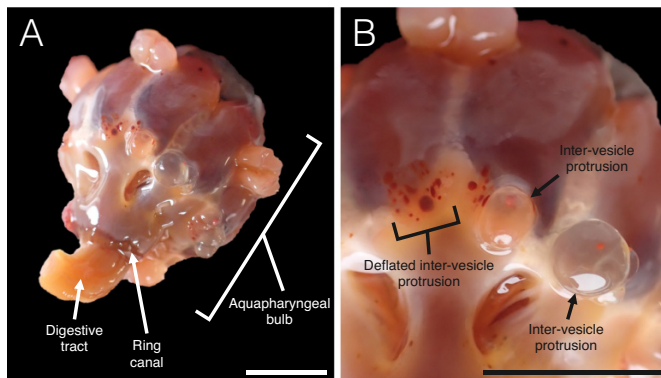
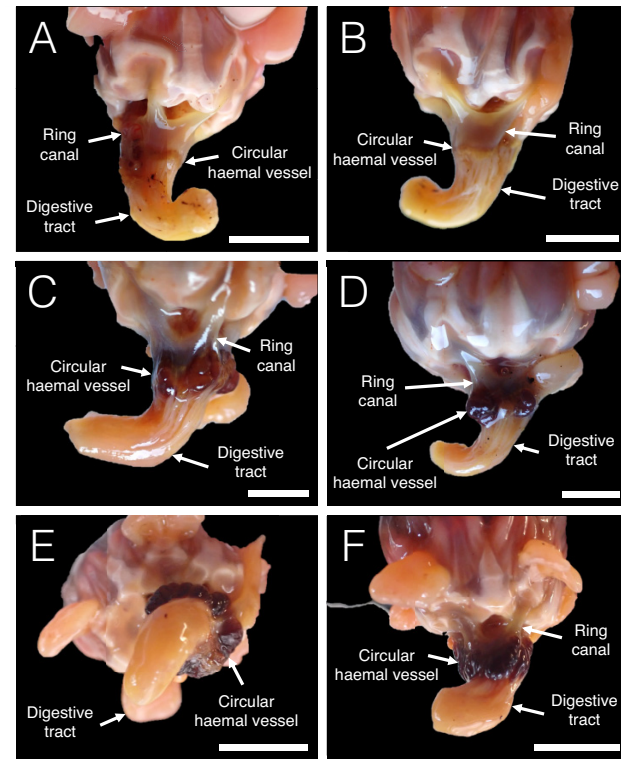


**Fig. 8.** Typical and atypical circular haemal vessel morphologies in the sea cucumber *Cucumaria frondosa* (Gunnerus, 1767): (A) left lateral view of a typical circular haemal vessel, (B) right lateral view of typical circular haemal vessel, (C and D) partially hypertrophied circular haemal vessel, and (E and F) completely hypertrophied circular haemal vessel; scale bars represent 20 mm.



the 12 protrusions totalled  $\sim$ 1.7 mL. The circulation of the hydrovascular fluid was bidirectional between the unaltered protrusions and the vesicles of the tentacles, which was not the case for deflated protrusions. Instead, these were filled with an abundance of coelomocytes, specifically morula cells ( $\sim$ 60%), filopodial phagocytes ( $\sim$ 20%), and few haemocytes forming light red aggregates. In contrast, the deflated protrusions were filled by a cumulative smaller quantity ( $\sim$ 0.1 mL) of hydrovascular fluid hosting an unusually large amount of haemocytes ( $\sim$ 50%) forming numerous dark red aggregates. Each protrusion was inspected but no foreign particles or parasites were found.

### Circular haemal vessel

During the dissection of the 94 specimens from the St. Pierre Bank collected between 2020 and 2021, four instances (4.2%) of hypertrophied circular vessels within the haemal system were discovered. The circular haemal vessel typically measured  $\sim$ 1 or 2 mm in width and encircled the very beginning of the stomach. The standard circular vessel lacked a developed lumen and contained very little fluid volume (Figs. 8A and 8B). In three of the abnormal individuals, the circular haemal vessels were found to be partially hypertrophied (Figs. 8C and 8D), while in the fourth, it was fully hypertrophied (Figs. 8E and 8F). The former varied in width from  $\sim$ 2 to 6 mm, while the latter was  $\sim$ 10 mm. Additionally, the hypertrophy seemed restricted to the circular haemal vessel, whereas the radial vessel around the digestive tract exhibited a normal size and morphology. Hypertrophied vessels hold a developed lumen of  $\sim$ 1–2 mm in diameter. These lumens were filled with a greater quantity of fluid containing coelomocytes and, more precisely, a higher density and number of haemocytes (data not shown).

### Discussion

The present study highlights that the morphological phenotype of *C. frondosa*, while superficially consistent, can vary strikingly both externally and internally. Some of these variations reflect expected deviations from the norm, whereas others exemplify clear abnormalities. Except for variations in the colour of the body wall and duplicated Polian vesicles reported in *C. frondosa* (Edwards 1910; Montgomery et al. 2019), all other atypical morphologies described herein are new to science, not only for the focal species but for holothuroids in general. In total, 1.3% of sea cucumbers examined displayed external variations and 15.9% displayed internal morphological variations. However, these proportions likely represent underestimations because the sea cucumbers were analysed opportunistically during different projects and by different researchers.

While the sea cucumbers examined here displayed a wide range of morphological variations and hypertrophied organs, none of them appeared to be visibly unhealthy. The dysmorphic features were all observed in adults, suggesting that none were severe enough to endanger the fitness/survival of the individuals, although it is still unclear whether they had any milder effect. The most striking abnormality involved

an individual displaying a bifurcated (split) posterior end, including part of the body wall, digestive tract, anus, and respective longitudinal muscles, while other individuals exhibited milder divided radial canals, duplicated rows of podia and ampullae as well as modified longitudinal and retractor muscle bands. A similar bifurcation of the body, but at the anterior end, was recently documented in five species of sea cucumbers by [Rupp et al. \(2024\)](#), who suggested it might be due to a genetic defect during development or be the result of incomplete fusion (chimerism) at the embryonic stage as reported by [Gianasi et al. \(2018\)](#).

Normal individuals of *C. frondosa* possess 10 tentacles linked to 10 vesicles. However, two individuals with 9 tentacles and one with 11 tentacles were found. The former still possessed 10 vesicles but one was atrophied, corresponding to the location of the missing tentacle. Despite a tentacle was missing and the lack of visible sign of non-lethal predation (i.e., scarring indicating tentacle loss), this abnormality likely emerged during regrowth after tentacle loss. As for the individual with 11 tentacles, it showed 11 vesicles with one vesicle that was hypertrophied, supporting morphologic defect during early development. In all cases, the tentacles were of equal size and they retracted, moved, and brought food to the mouth in a similar pattern as the 10 tentacles of typical individuals (K.C.K. Ma, personal observation).

The protrusions observed at the base of some of the vesicle of the tentacles and the hypertrophied circular haemal vessel might be non-permanent abnormalities potentially caused by a momentary immunological response. It could be the results of the accumulation of coelomocytes or an inflammatory reaction of connective tissues to counteract an infection by microorganisms, as already suggested by [Jangoux \(1987\)](#) while describing the consequence of diseases in other echinoderms. When deflated, the protrusions were filled with proportionally more coelomocyte aggregates than seen in other hydrovascular fluids examined. This observation is in line with the reactions of the ring canal reported in *Holothuria (Roweothuria) poli* Delle Chiaje, 1824 following antigenic injection aiming to stimulate the immune system by [Lunetta and Michelucci \(2002\)](#). Similarly, haemocytes were shown to spike in various fluids (as individual cells or aggregates) when *C. frondosa* was exposed to adverse conditions, while they are virtually absent under stable conditions ([Caulier et al. 2020, 2024; Hamel et al. 2021; Jobson et al. 2022](#)). Therefore, recruitment of haemocytes in the deflated inter-vesicle protrusion potentially reflected an immune reaction that included the expansion of connective tissues to isolate pathogens (there is no fluid exchange between deflated protrusions and the tentacular vesicle). Despite no pathogens were observed in the present analysis, the high abundance of coelomocytes could suggest that they already had been eliminated/aggregated. The typical circular vessel of Dendrochiro-rotida is thin with a small lumen containing fluid and free-swimming cells ([Burton 1964; Fish 1967](#)). The hypertrophy of the vessel in the present study was associated with a larger lumen filled with an important number of haemocytes. The recruitment of these immune cells suggests that the hypertrophy might be driven by a pathogenic infection leading to an immune response or brown-tissue degeneration tumour-like

reaction, as already described in *Holothuria leucospilota* ([Smith et al. 1973](#)).

[Edwards \(1910\)](#) mentioned that 6% of individuals of *C. frondosa* in his study exhibited a second “accessory” Polian vesicle. It is worth noting that the proportion of the sampled population with more than one Polian vesicle noted here was similar (6.8% in the population from Tors Cove and 6.4% in the population from the St. Pierre Bank), suggesting that this is the normal rate of variability in the species. This phenomenon is likely to be geographically widespread given that it is consistently observed throughout the species’ range, including in Arctic populations sampled in Qikiqtait, Nunavut, Canada (K.C.K. Ma, personal observation). Additionally, novel insight of the consistent positioning of the second Polian vesicle’s insertion point on the ring canal suggests a predisposition for Polian vesicles to be located on the right ventral inter-radius, indicating potential phenotypic plasticity. *Cucumaria miniata* (Brandt, 1835), which has also been described to occasionally possess more than one Polian vesicle, does not manifest a tendency as clear as *C. frondosa*, since its second and third Polian vesicle shift from the ventral left, ventral right, and dorsal right inter-radius ([Edwards 1910](#)). The novelty of the present study was the observation of multiple Polian vesicles (>2), as well as split vesicles in some individuals. It was suggested by [Caulier et al. \(2020\)](#) and [Hamel et al. \(2021\)](#) that flushing the coelomocyte aggregates into the perivisceral coelom from the hydrovascular system and the active buoyancy adjustment, respectively, involved vesicle rupture to some degree, requiring reconstruction of this organ on a regular basis. These reconstructions could be generating splits at the point of rupture or, if the damage is too severe, might require the development of new vesicles to maintain appropriate fluid volumes in the hydrovascular system. Given that the tissue composing Polian vesicles is hematopoietic, it could allow the production of immunological agents. It is possible that increased surface area through multiple or lobed vesicles would provide an evolutionary immunological advantage ([Canicatti et al. 1989; Levin and Gudimova 1997; Cayabo and Mabuhay-Omar 2016; Li et al. 2019; Caulier et al. 2020; Shi et al. 2020; Guo et al. 2021](#)). The Polian vesicle(s) is/are essential for extension and contraction of podia and tentacles ([Li et al. 2013](#)) and plays/play a role in excretory and immunology ([Baccetti and Rosati 1968; Lawrence 2001; Caulier et al. 2020](#)), emphasising its/their importance.

Although some descriptions of the stone canal of *C. frondosa* have been presented in the past ([Edwards 1910; Levin and Gudimova 1997](#)), no morphological variations of this organ have ever been documented. While most sea cucumbers have only one internalised stone canal ([Hyman 1955; Erber 1983](#)), some species can have more, such as *Holothuria (Roweothuria) arguinensis* Koehler & Vaney, 1906 (6–11 stone canals with equivalent number of madreporite associated) and *Holothuria atra* Jaeger, 1833 (1–18 stone canals with equivalent number of madreporite associated) ([Tehranifard and Rahimibashar 2012; Mezali and Thandar 2014](#)). However, only one stone canal was described and characterised in *C. frondosa*. Here, in all individuals examined, the stone canal was consistent with original descriptions, but the madreporite in some sea cucumbers was hypertrophied or multiplied. The function and

benefit of the madreporite are mostly considered as vestigial in Holothuroidea (Erber 1983), making it difficult to evaluate the impact of the hypertrophied madreporite on the fitness of the sea cucumber. The driver of this abnormality is also difficult to evaluate but since this organ cannot regenerate (Delage 1902), it is unlikely to result from damage and subsequent healing.

As information about morphological variations and dysmorphic features in echinoderms is still emerging, it is challenging to identify the underlying drivers with any certainty. Most documented cases of morphological variation or abnormality in Echinodermata, including in Holothuroidea, arose during embryonic-larval development following exposure to heavy metals or antifouling pollutants (Warnau et al. 1996; Pesando et al. 2003; Moureaux et al. 2011; Carballera et al. 2012; Morroni et al. 2023). Consequently, the dysmorphic features detailed in the present study could potentially result from exposure to toxic waste or teratogens, even though it is unlikely to occur given the relatively remote/pristine locations from which most of them were sampled. These anomalies are more plausibly driven by disease, spontaneous mutation, atypical regeneration process, and, to a lesser extent, fluctuations in salinity and temperature, or pathogens (Hotchkiss 1979; Watts et al. 1983; Jangoux 1987; Vergneau-Grosset et al. 2022). In addition, these abnormalities may have emerged at various developmental stages, including during the larval development (e.g., X- and Y-longitudinal muscle bands and bifurcated posterior end) or possibly at the adult stage (e.g., aquapharyngeal protrusions and hypertrophied haemal vessel). Arguably, malformations might be an indicator of shifts in environmental conditions.

Perspectives of future research on this topic may include more detailed observations of the microstructure of the dysmorphic variations and potential cellular alterations by scanning/transmission electronic microscopy and cytomorphological analyses (Sugni et al. 2007; Núñez-Pons et al. 2018; Peters 2021). In addition to cellular observations, impact on molecular mechanisms and metabolite variations could be explored using mass spectroscopy, metabolomics, and molecular biology (Capello et al. 2017; Ruocco et al. 2018; Silva et al. 2019; Lu et al. 2022). Further analyses monitoring the rate of morphological variations and abnormalities would help to assess population, and potentially ecosystem health. Studies comparing additional populations across various locations, alongside analyses of the physico-chemical parameters of their tissues and surrounding water, would provide potential valuable insights into the influence of these parameters and general environmental impact. Moreover, next-generation sequencing and transcriptomic analysis could yield important information on heritability, rate of divergence, and genetic variations to complete our understanding of morphological plasticity and dysmorphology in echinoderms.

The present contribution offers the first inventory of dysmorphic features for an echinoderm species, describing seven completely new variations and abnormalities in *C. frondosa* and six novelties in the class Holothuroidea. Overall, findings provide insights into the diversity of external and internal morphologies in this species and bridges gaps in the literature by comparing typical and atypical morphologies of

tissues and organs under investigation. It also emphasises the notable rate of internal abnormalities in certain populations and the fact that morphological variations or abnormalities should be more consistently reported in the literature, otherwise their occurrence and drivers may be overlooked. Understanding the environmental, biological, or genetic drivers of these abnormalities would yield crucial data for research in areas such as immune function, regeneration, and ecotoxicology and provide a deeper understanding of the function of affected organs.

## Acknowledgements

Sea cucumbers used in this study were either collected by the Field Services of the Department of Ocean Sciences, Memorial University, or provided by Quin-Sea Fisheries Ltd., a division of Royal Greenland. We thank Sophie Wolvin, Robert Trenholm, Qiang Xu, and employees at Quin-Sea for their assistance at the processing plant in Cape Broyle and Heather D. Penney for her assistance in the laboratory. This study was partly supported by funding from Mitacs Accelerate (IT15224 and IT29594), the Newfoundland sea cucumber industry, WWF-Canada, and the Natural Sciences and Engineering Research Council of Canada (NSERC) to AM.

## Article information

### History dates

Received: 23 January 2025

Accepted: 31 March 2025

Accepted manuscript online: 28 June 2025

Version of record online: 2 September 2025

### Copyright

© 2025 The Authors. Permission for reuse (free in most cases) can be obtained from [copyright.com](https://copyright.com).

### Data availability

Data generated or analysed during this study are provided in full within the published article.

## Author information

### Author ORCIDs

Guillaume Corbisier <https://orcid.org/0009-0002-7459-8650>

### Author contributions

Conceptualization: GC, KCKM, SMJ, JH, GC, AM

Data curation: GC, KCKM, SMJ

Formal analysis: GC, KCKM, SMJ

Funding acquisition: AM

Investigation: GC, KCKM, SMJ

Methodology: GC, KCKM, SMJ, JH

Project administration: JH, GC, AM

Supervision: JH, GC, AM

Validation: JH, GC, AM

Visualization: JH, AM

Writing – original draft: GC, KCKM, SMJ  
 Writing – review & editing: GC, KCKM, SMJ, JH, GC, AM

## Competing interests

The authors declare there are no competing interests.

## References

Adamski, Z., Niewadzi, M., and Ziernicki, K. 2005. Inheritance of chorionic malformations and insecticide resistance by *Spodoptera exigua*. *J. Appl. Entomol.* **129**(9–10): 526–533. doi:10.1111/j.1439-0418.2005.01001.x.

Allain, J.Y. 1978. Déformations du test chez l'oursin *Lytechinus variegatus* (Lamarck) (Echinoidea) de la baie de Carthagène. *Caldasia*, **12**(58): 363–375.

Baccetti, B., and Rosati, F. 1968. The fine structure of the Polian vesicles of holothurians. *Zeitschr. Zellforsch. Mikroskop. Anat.* **90**(1): 148–160. doi:10.1007/BF00496708.

Burton, M.P.M. 1964. Haemal system of regular echinoids. *Nature*, **204**: 1218–1218. doi:10.1038/2041218a0. PMID: 14264397.

Candia Carnevali, M.D. 2005. Regenerative response and endocrine disrupters in crinoid echinoderms: an old experimental model, a new ecotoxicological test. *Prog. Mol. Subcell. Biol.* **39**: 167–200. doi:10.1007/3-540-27683-1\_8. PMID: 17152698.

Canicattì, C., D'Ancona, G., and Farina-Lipari, E. 1989. The coelomocytes of *Holothuria polii* (Echinodermata). I. Light and electron microscopy. *Bullet. Zool.* **56**(1): 29–36. doi:10.1080/11250008909355618.

Cappello, T., Vitale, V., Oliva, S., Villari, V., Mauceri, A., Fasulo, S., and Maisano, M. 2017. Alteration of neurotransmission and skeletogenesis in sea urchin *Arbacia lixula* embryos exposed to copper oxide nanoparticles. *Comp. Biochem. Physiol. C Toxicol. Pharmacol.* **199**: 20–27. doi:10.1016/j.cbpc.2017.02.002. PMID: 28188896.

Carballeira, C., Ramos-Gómez, J., Martín-Díaz, L., and DelValls, T.A. 2012. Identification of specific malformations of sea urchin larvae for toxicity assessment: application to marine pisciculture effluents. *Mar. Environ. Res.* **77**: 12–22. doi:10.1016/j.marenvres.2012.01.001. PMID: 22341183.

Caulier, G., Hamel, J-F., and Mercier, A. 2020. From coelomocytes to colored aggregates: cellular components and processes involved in the immune response of the holothuroid *Cucumaria frondosa*. *Biol. Bull.* **239**(2): 95–114. doi:10.1086/710355. PMID: 33151755.

Caulier, G., Jobson, S., Wambreuse, N., Borrello, L., Delroisse, J., Eeckhaut, I., et al. 2024. Vibratile cells and hemocytes in sea cucumbers—clarifications and new paradigms. In *The world of sea cucumbers*. Vol. 1. Academic Press. pp. 403–412. doi:10.1016/B978-0-323-95377-1.00024-2.

Cayabo, G.D.B., and Mabuhay-Omar, J.A. 2016. Antibacterial potential of crude extracts from sea cucumber *Holothuria fuscoscincerea* Jaeger, 1833. *Palawan Sci.* **8**: 47–61. doi:10.69721/TPS.J.2016.08.1.04.

Claes, P., Daniels, K., Walters, M., Clement, J., Vandermeulen, D., and Suetens, P. 2012. Dysmorphometrics: the modelling of morphological abnormalities. *Theor. Biol. Med.* **9**: 1–28. doi:10.1186/1742-4682-9-5.

Dafni, J. 1980. Abnormal growth patterns in the sea urchin *Tripneustes cf. gratilla* (L.) under pollution (Echinodermata, Echinoidea). *J. Exp. Mar. Biol. Ecol.* **47**(3): 259–279. doi:10.1016/0022-0981(80)90043-X.

Delage, Y. 1902. Effets de l'excision du madréporite chez les astéries. *CR Acad. Sci. (Paris)*, **135**: 841–842.

Edwards, C.L. 1910. Four species of Pacific Ocean holothurians allied to *Cucumaria frondosa* (Gunner). *Zool. Jahrb. Abt. F. Syst. Bd.* **29**: 597–612.

Eeckhaut, I., and Améziane-Cominardi, N. 2020. Structural description of three myzostomes parasites of crinoids and of the skeletal deformations they induce on their hosts. In *Echinoderms through time*. CRC Press, pp. 203–209. doi:10.1201/9781003077831-39.

Erber, V.W. 1983. Der Steinkanal der Holothurien: eine morphologische studie zum problem der protocoelampulle 1. *J. Zool. Syst. Evol. Res.* **21**(3): 217–235. doi:10.1111/j.1439-0469.1983.tb00289.x.

Fish, J.D. 1967. The digestive system of the holothurian, *Cucumaria elongata*. I. Structure of the gut and hemal system. *Biol. Bull.* **132**(3): 337–353. doi:10.2307/1539639.

Flandroit, A., Simon, L., and Caulier, G. 2024. Description of limb anomalies resulting from molt irregularities in *Ammothaea hilgendorfi* (Py-cnogonida: Ammotheidae). *Arthropoda*, **2**(2): 156–168. doi:10.3390/arthropoda2020012.

Fontaine, A.R. 1969. Pigmented tumor-like lesions in an ophiuroid echinoderm. *J. Natl. Cancer Inst.* **31**: 255–261.

Galván-Villa, C.M., and Solís-Marín, F.A. 2021. Population size structure and abnormalities in the number of rays of the Sea Star *Pentaceraster cumingi* (Valvatida: Oreasteridae) in Bahía Chamela, Mexican Pacific. *Rev. Biol. Trop.* **69**(1): 262–273. doi:10.15517/rbt.v69i1.43239.

Gianasi, B.L., Hamel, J-F., and Mercier, A. 2018. Full allogeneic fusion of embryos in a holothuroid echinoderm. *Proc. R. Soc. B Biol. Sci.* **285**(1879): 20180339. doi:10.1098/rspb.2018.0339.

Gianasi, B.L., Hamel, J-F., Montgomery, E.M., Sun, J., and Mercier, A. 2021. Current knowledge on the biology, ecology, and commercial exploitation of the sea cucumber *Cucumaria frondosa*. *Rev. Fish. Sci. Aquacult.* **29**(4): 582–653. doi:10.1080/23308249.2020.1839015.

Guo, L., Wang, Z., Shi, W., Wang, Y., and Li, Q. 2021. Transcriptome analysis reveals roles of polian vesicle in sea cucumber *Apostichopus japonicus* response to *Vibrio splendidus* infection. *Comp. Biochem. Physiol. D Genom. Proteom.* **40**: 100877. doi:10.1016/j.cbd.2021.100877.

Hamel, J.-F., and Mercier, A. 1996. Gonad morphology and gametogenesis of the sea cucumber *Cucumaria frondosa*. *SPC Beche-de-mer Inf. Bull.* **40**: 22–33.

Hamel, J.-F., Jobson, S., Caulier, G., and Mercier, A. 2021. Evidence of anticipatory immune and hormonal responses to predation risk in an echinoderm. *Sci. Rep.* **11**(1): 10691. doi:10.1038/s41598-021-89805-0. PMID: 34021182.

Hawkins, H.L. 1917. I. Morphological studies on the Echinoidea Holothopoda and their allies. *Geol. Mag.* **57**(10): 433–441. doi:10.1017/S0016756800106600.

Hossain, A., Dave, D., and Shahidi, F. 2020. Northern sea cucumber (*Cucumaria frondosa*): a potential candidate for functional food, nutraceutical, and pharmaceutical sector. *Mar. Drugs*, **18**(5): 274. doi:10.3390/med18050274. PMID: 32455954.

Hotchkiss, F.H. 1979. Case studies in the teratology of starfish. *Proc. Acad. Nat. Sci. Philadelphia*, **131**: 139–157.

Hyman, L.H. 1955. The invertebrates: Echinodermata, the coelomate bilateria 4. McGraw-Hill book Company Inc., New York. p. 783.

Jangoux, M. 1987. Diseases of echinodermata. IV. Structural abnormalities and general considerations on biotic diseases. *Dis. Aquat. Organ.* **3**(3): 221–229. doi:10.3354/dao003221.

Jobson, S., Hamel, J-F., and Mercier, A. 2022. Rainbow bodies: revisiting the diversity of coelomocyte aggregates and their synthesis in echinoderms. *Fish Shellfish Immunol.* **122**: 352–365. doi:10.1016/j.fsi.2022.02.009.

Lawrence, J.M. 2001. Function of eponymous structures in echinoderms: a review. *Can. J. Zool.* **79**(7): 1251–1264. doi:10.1139/cjz-79-7-1251.

Leśniewska, M., Bonato, L., Minelli, A., and Fusco, G. 2009. Trunk anomalies in the centipede *Stigmatogaster subterranea* provide insight into late-embryonic segmentation. *Arthropod Struct. Dev.* **38**(5): 417–426. doi:10.1016/j.asd.2009.05.001.

Levin, V.S., and Gudimova, E.N. 1997. Taxonomic interrelations of holothurians *Cucumaria frondosa* and *C. japonica* (Dendrochirotida, Cucumariidae). *SPC Beche-de-Mer Inf. Bull.* **13**: 22–29.

Li, Q., Qi, R.R., Wang, Y.N., Ye, S.G., Qiao, G., and Li, H. 2013. Comparison of cells free in coelomic and water-vascular system of sea cucumber, *Apostichopus japonicus*. *Fish & Shellfish Immunol.* **35**(5): 1654–1657. doi:10.1016/j.fsi.2013.07.020.

Li, Q., Ren, Y., Luan, L., Zhang, J., Qiao, G., Wang, Y., et al. 2019. Localization and characterization of hematopoietic tissues in adult sea cucumber, *Apostichopus japonicus*. *Fish Shellfish Immunol.* **84**: 1–7. doi:10.1016/j.fsi.2018.09.058.

Lu, L., Ren, L., Jiang, L., Xu, X., Wang, W., Feng, Y., et al. 2022. Integrative proteomics and metabolomics reveal the stress response of semicarbazide in the sea cucumber *Apostichopus japonicus*. *Front. Mar. Sci.* **9**: 992753. doi:10.3389/fmars.2022.992753.

Lunetta, G.D.A., and Michelucci, M.L. 2002. Engagement of the periesophageal ring during *Holothuria polii* response to erythrocyte injection. *Eur. J. Histochem.* **46**(2): 185–194. doi:10.4081/1669.

Malcomson, R.O. 1953. Arthropod teratology. *Can. Entomol.* **85**(9): 313–315. doi:10.4039/Ent85313-9.

McEuen, F.S. 1988. Spawning behaviors of northeast Pacific sea cucumbers (Holothuroidea: Echinodermata). *Mar. Biol.* **98**(4): 565–585. doi:[10.1007/BF00391548](https://doi.org/10.1007/BF00391548).

Mercier, A., Penney, H.D., Ma, K.C.K., Lovatelli, A., and Hamel, J.-F. 2023. A guide to northern sea cucumbers: the biology and management of *Cucumaria frondosa*. FAO Fish. Aquac. Tech. Pap., 700. FAO, Rome. pp. xvii + 92. doi:[10.4060/cc7928en](https://doi.org/10.4060/cc7928en).

Mezali, K., and Thandar, A.S. 2014. First record of *Holothuria (Roweothuria) arguinensis* (echinodermata: holothuroidea: aspidochirotiida: holothuriidae) from the Algerian coastal waters. *Mar. Biodivers. Rec.* **7**(40): 1–4. doi:[10.1017/S1755267214000438](https://doi.org/10.1017/S1755267214000438).

Mironov, A.N., Minin, K.V., and Dilman, A.B. 2015. Abyssal echinoid and asteroid fauna of the North Pacific. *Deep Sea Res. Part II*, **111**: 357–375. doi:[10.1016/j.dsr2.2014.08.006](https://doi.org/10.1016/j.dsr2.2014.08.006).

Montgomery, E.M., Ferguson-Roberts, J.M., Gianasi, B.L., Hamel, J.-F., Kremenetskaia, A., and Mercier, A. 2018. Functional significance and characterization of sexual dimorphism in holothuroids. *Invertebr. Reprod. Dev.* **62**(4): 191–201. doi:[10.1080/07924259.2018.1491898](https://doi.org/10.1080/07924259.2018.1491898).

Montgomery, E.M., Small, T., Hamel, J.-F., and Mercier, A. 2019. Albinism in orange-footed sea cucumber (*Cucumaria frondosa*) in Newfoundland. *Can. Field-Nat.* **133**(2): 113–117. doi:[10.22621/cfn.v133i2.2047](https://doi.org/10.22621/cfn.v133i2.2047).

Morroni, L., Rakaj, A., Grosso, L., Fianchini, A., Pellegrini, D., and Regoli, F. 2020. Sea cucumber *Holothuria polii* (Delle Chiaje, 1823) as new model for embryo bioassays in ecotoxicological studies. *Chemosphere*, **240**: 124819. doi:[10.1016/j.chemosphere.2019.124819](https://doi.org/10.1016/j.chemosphere.2019.124819).

Morroni, L., Rakaj, A., Grosso, L., Flori, G., Fianchini, A., Pellegrini, D., and Regoli, F. 2023. Echinoderm larvae as bioindicators for the assessment of marine pollution: sea urchin and sea cucumber responsiveness and future perspectives. *Environ. Pollut.* **335**: 122285. doi:[10.1016/j.envpol.2023.122285](https://doi.org/10.1016/j.envpol.2023.122285).

Moureaux, C., Simon, J., Mannaerts, G., Catarino, A.I., Pernet, P., and Dubois, P. 2011. Effects of field contamination by metals (Cd, Cu, Pb, Zn) on biometry and mechanics of echinoderm ossicles. *Aquat. Toxicol.* **105**(3–4): 698–707. doi:[10.1016/j.aquatox.2011.09.007](https://doi.org/10.1016/j.aquatox.2011.09.007).

Nelson, E.J., MacDonald, B.A., and Robinson, S.M. 2012. A review of the Northern Sea cucumber *Cucumaria frondosa* (Gunnerus, 1767) as a potential aquaculture species. *Rev. Fish. Sci.* **20**(4): 212–219. doi:[10.1080/10641262.2012.719043](https://doi.org/10.1080/10641262.2012.719043).

Núñez-Pons, L., Work, T. M., Angulo-Preckler, C., Moles, J., and Avila, C. 2018. Exploring the pathology of an epidermal disease affecting a circum-Antarctic sea star. *Sci. Rep.* **8**(1): 11353. doi:[10.1038/s41598-018-29684-0](https://doi.org/10.1038/s41598-018-29684-0).

O'Loughlin, P. 2001. The occurrence and role of a digitate genital papilla in holothurian reproduction. In *Echinoderms 2000*. pp. 363–368.

Pesando, D., Huitorel, P., Dolcini, V., Angelini, C., Guidetti, P., and Falugi, C. 2003. Biological targets of neurotoxic pesticides analysed by alteration of developmental events in the Mediterranean Sea urchin, *Paracentrotus lividus*. *Mar. Environ. Res.* **55**(1): 39–57. doi:[10.1016/s0141-1136\(02\)00215-5](https://doi.org/10.1016/s0141-1136(02)00215-5).

Peters, E.C. 2021. Diseases of other invertebrate phyla: Porifera, Cnidaria, Ctenophora, Annelida, Echinodermata. In *Pathobiology of marine and estuarine organisms*. CRC press. pp. 393–449. doi:[10.1201/9781003069058-15](https://doi.org/10.1201/9781003069058-15).

Roman, J. 1952. Quelques anomalies chez *Clypeaster melitensis* Michelin. *Bull. Soc. Géol. France*, **S6-II**(1–3): 3–11. doi:[10.2113/gssgbull.S6-II.1-3.3](https://doi.org/10.2113/gssgbull.S6-II.1-3.3).

Roux, M., and Philippe, M. 2021. Early Miocene stalked crinoids (Echinodermata) from the southern Rhodanian Basin (southeastern France). *Paleoenvironments and taxonomy. Zootaxa*, **5052**(3): 301–331. doi:[10.11646/zootaxa.5052.3.1](https://doi.org/10.11646/zootaxa.5052.3.1).

Ruocco, N., Costantini, S., Zupo, V., Lauritano, C., Caramiello, D., Ianora, A., et al. 2018. Toxicogenic effects of two benthic diatoms upon grazing activity of the sea urchin: morphological, metabolomic and de novo transcriptomic analysis. *Sci. Rep.* **8**(1): 5622. doi:[10.1038/s41598-018-24023-9](https://doi.org/10.1038/s41598-018-24023-9).

Rupp, G.S., Martins, L., Souto, C., Hamel, J.-F., and Mercier, A. 2024. Morphological characterization of anterior axial bifurcation in *Holothuria (Halodeima) grisea* and other puzzling occurrences in Holothuroidea. *Invertebr. Biol.* **143**(3): e12434. doi:[10.1111/ivb.12434](https://doi.org/10.1111/ivb.12434).

Saint-Seine, R.D. 1950. Lésions et régénération chez le Micraster. *Bull. Soc. Géol. France*, **S5-XX**(7–9): 309–315. doi:[10.2113/gssgbull.S5-XX.7-9.309](https://doi.org/10.2113/gssgbull.S5-XX.7-9.309).

Scholtz, G. 2020. Duplicated, twisted, and in the wrong place: patterns of malformation in crustaceans. In *Developmental biology and larval ecology: the natural history of the Crustacea*, 7. pp. 112–142. doi:[10.1093/oso/9780190648954.003.0004](https://doi.org/10.1093/oso/9780190648954.003.0004).

Serafy, D.K. 1971. Intraspecific variation in the brittle-star *Ophiopholis aculeata* (Linnaeus) in the northwestern Atlantic (Echinodermata; Ophiuroidea). *Biol. Bull.* **140**(2): 323–330. doi:[10.2307/1540076](https://doi.org/10.2307/1540076).

Shi, W., Zhang, J., Wang, Y., Ji, J., Guo, L., Ren, Y., et al. 2020. Transcriptome analysis of sea cucumber (*Apostichopus japonicus*) Polian vesicles in response to evisceration. *Fish Shellfish Immunol.* **97**: 108–113. doi:[10.1016/j.fsi.2019.12.016](https://doi.org/10.1016/j.fsi.2019.12.016).

Silva, M.S., Sele, V., Sloth, J.J., Araujo, P., and Amlund, H. 2019. Speciation of zinc in fish feed by size exclusion chromatography coupled to inductively coupled plasma mass spectrometry—using fractional factorial design for method optimisation and mild extraction conditions. *J. Chromatogr. B*, **1104**: 262–268. doi:[10.1016/j.jchromb.2018.11.010](https://doi.org/10.1016/j.jchromb.2018.11.010).

Smith, A.C., Taylor, R.L., Chun-Akana, H., and Ramos, F. 1973. Intestinal tumor in the sea cucumber, *Holothuria leucospilota*. *J. Invertebr. Pathol.* **22**(2): 305–307. doi:[10.1016/0022-2011\(73\)90154-7](https://doi.org/10.1016/0022-2011(73)90154-7).

Sparks, A. 2012. *Invertebrate pathology noncommunicable diseases*. Elsevier, Academic Press.

Stewart, B.G., and Mladenov, P.V. 1997. Population structure, growth and recruitment of the euryalnid brittle-star *Astrobrachion constrictum* (Echinodermata: Ophiuroidea) in Doubtful Sound, Fiordland, New Zealand. *Mar. Biol.* **127**: 687–697. doi:[10.1007/s002270050059](https://doi.org/10.1007/s002270050059).

Stiller, F. 1999. Phenotypic variability, deformations and post-traumatic reactions of the stem of *Encribus cf. liliiformis* Lamarck (Crinoidea) from the Middle Triassic of Qingyan, south-western China. *Paläontol. Zeitschr.* **73**(3): 303–318. doi:[10.1007/BF02988042](https://doi.org/10.1007/BF02988042).

Sugni, M., Mozzi, D., Barbaglio, A., Bonasoro, F., and Candia Carnevali, M.D. 2007. Endocrine disrupting compounds and echinoderms: new ecotoxicological sentinels for the marine ecosystem. *Front. Mar. Sci.* **9**: 95–108. doi:[10.3389/fmars.2022.992753](https://doi.org/10.3389/fmars.2022.992753).

Tehranifarid, A., and Rahimibashar, M.R. 2012. Description a sea cucumber species *Holothuria atra* Jaeger, 1833 from Kiss Island Iran (Echinodermata: Holothuroidea). *J. Bas. Appl. Sci. Res.* **2**(12): 12660–12662.

Thomka, J.R., Malgieri, T.J., and Brett, C.E. 2014. A swollen crinoid pluricolumnal from the Upper Ordovician of northern Kentucky, USA: the oldest record of an amorphous paleopathologic response in Crinoidea? *Eston. J. Earth Sci.* **63**(4): 317–322. doi:[10.3176/earth.2014.37](https://doi.org/10.3176/earth.2014.37).

Utinomi, H. 1971. Records of Pycnogonida from shallow waters of Japan. *Publications Seto Mar. Biol. Lab.* **18**(5): 317–347. doi:[10.5134/175643](https://doi.org/10.5134/175643).

Vergneau-Grosset, C., Boudreau, R., Favoretto, F., Beauchamp, G., Chicoine, A.J., Sánchez, C., and Doucet, M.Y. 2022. Occurrence of ulcerative lesions in sea stars (Asteroidea) of the Northern Gulf of California, Mexico. *J. Wildl. Dis.* **58**(1): 215–221. doi:[10.7589/JWD-D-21-00044](https://doi.org/10.7589/JWD-D-21-00044).

Wang, H., Liu, H., Zhang, Y., Zhang, L., Wang, Q., and Zhao, Y. 2023. The toxicity of microplastics and their leachates to embryonic development of the sea cucumber *Apostichopus japonicus*. *Mar. Environ. Res.* **190**: 106114. doi:[10.1016/j.marenvres.2023.106114](https://doi.org/10.1016/j.marenvres.2023.106114).

Warnau, M., Temara, A., Jangoux, M., Dubois, P., Iaccarino, M., De Biase, A., and Pagano, G. 1996. Spermiotoxicity and embryotoxicity of heavy metals in the echinoid *Paracentrotus lividus*. *Mar. Environ. Res.* **190**(11): 1931–1936. doi:[10.1016/j.marenvres.2023.106114](https://doi.org/10.1016/j.marenvres.2023.106114).

Watts, S.A., Scheibling, R.E., Marsh, A.G., and McClintock, J.B. 1983. Induction of aberrant ray numbers in *Echinaster* sp. (Echinodermata: Asteroidea) by high salinity. *Florida Sci.* **46**(2): 125–128.

Whitman, D.W., and Agrawal, A.A. 2009. What is phenotypic plasticity and why is it important. In *Phenotypic plasticity of insects: mechanisms and consequences*. pp. 1–63. doi:[10.1201/b10201](https://doi.org/10.1201/b10201).

Xing, L., Sun, L., and Huo, D. 2024. Color morphs in *Apostichopus japonicus*: physiology and molecular regulation mechanisms. In *The world of sea cucumbers*. Academic Press. pp. 547–564. doi:[10.1016/B978-0-323-95377-1.00039-4](https://doi.org/10.1016/B978-0-323-95377-1.00039-4).

Xu, E.G., Morton, B., Lee, J.H., and Leung, K.M. 2015. Environmental fate and ecological risks of nonylphenols and bisphenol A in the Cape D'Aguilar Marine Reserve, Hong Kong. *Mar. Pollut. Bull.* **91**(1): 128–138. doi:[10.1016/j.marpolbul.2014.12.017](https://doi.org/10.1016/j.marpolbul.2014.12.017).

Copyright of Canadian Journal of Zoology is the property of Canadian Science Publishing and its content may not be copied or emailed to multiple sites or posted to a listserv without the copyright holder's express written permission. However, users may print, download, or email articles for individual use.